cAMP generation by $PGE_2$-EP2/EP4 signalling[9] combined with that by CD28 costimulation can cancel out the cAMP-mediated inhibition of TCR signalling, and preserve, for example, expression of critical genes such as CD25, IL-2 and IFN-γ. The primary inhibitory site by cAMP may be Lck. Tasken and his collaborators suggested that PKA interferes with LCK activation, and this action can be antagonized by PI3K activation following CD28 costimulation[33,40].

Then, how important is this $PGE_2$-cAMP-dependent mechanism in Th1-mediated immune response *in vivo* and in human immune diseases? Here we have used two disease models and demonstrated that EP4-cAMP signalling in T cells facilitated expression of Th1 cytokine receptors and Th1 response *in vivo*. We have generated mice with selective deletion of EP4 in T cells, and revealed that the loss of EP4 in T cells considerably attenuates CHS response and the adoptive transfer colitis. In both models, selective blockade of EP4 in T cells prevented *in vivo* Th1 differentiation with downregulated expression of *Il12rb2*, *Ifngr1* and *Il2rb* genes and other CREB/CRTC2-dependent genes in lymph nodes (LNs) $CD4^+$ T cells. CHS is a mouse model of allergic contact dermatitis in humans, in which IFN-γ produced by $CD4^+$ Th1 and $CD8^+$ type 1 cytotoxic T cells has an important role[41]. The adoptive transfer colitis is a model of inflammatory bowel disease, particularly CD[42]. Genome-wide association studies have revealed that the *PTGER4*, *IL12RB2* and *IL2RA* (human IL-2Rα) genes are linked to risk loci associated with CD[13,14]. High expression of *IL12RB2*, *IL2RA* and *IL2RB* (encoding human IL-2Rβ) genes was found in blood or in lamina propria $CD4^+$ T cells of patients with CD[43,44]. Upregulation of CREB was also found in peripheral blood mononuclear cells from patients with inflammatory diseases including CD[45]. Additionally, in experimental allergic encephalomyelitis, a mouse model for multiple sclerosis, systemic inhibition of EP4 suppressed Th1 differentiation and IFN-γ production[9,46]. Interestingly, *PTGER4* and *IL12RB2* were shown to be associated with multiple sclerosis[12,15]. Thus, our results showed that EP4-cAMP signalling in T cells has a critical role in regulation of cytokine signalling and Th1 response *in vivo* using various mouse models of immune inflammation and suggest the possibility of similar actions operating clinically in human diseases.

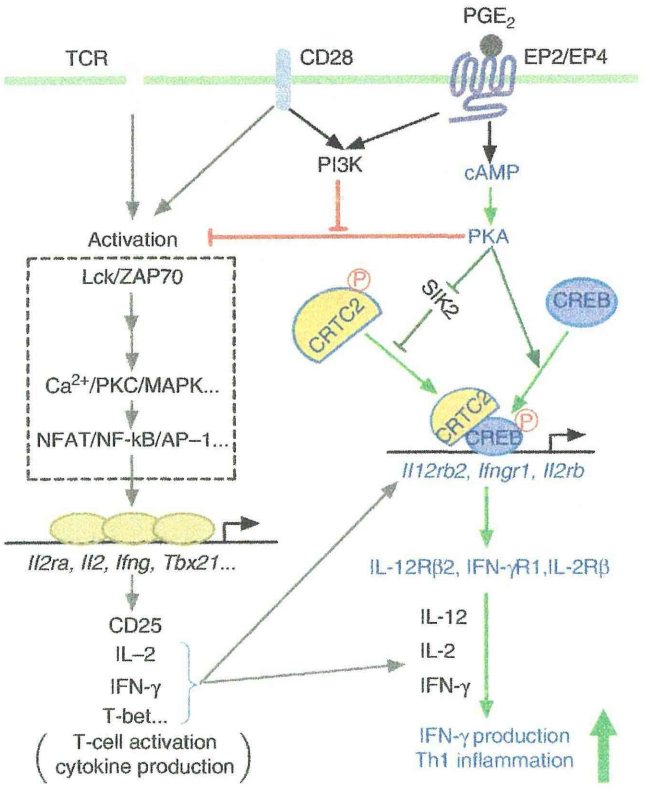


**Figure 8 | A model for synergistic action of cAMP and PI3K in Th1 differentiation.** cAMP generated in response to $PGE_2$ binding to EP2/EP4 activates PKA, which phosphorylates CREB and activates CRTC2 through phosphorylation of SIK. Activated CREB and CRTC2 translocate to the nucleus and induce expression of *Il12rb2*, *Ifngr1* and possibly *Il2rb*, thus facilitating Th1 differentiation synergistically with IL-12, IFN-γ and IL-2. While cAMP-PKA inhibits T-cell activation by suppressing TCR signalling, coactivation of PI3K by EP2/EP4 and CD28 cancels this inhibition and promotes the Th1-facilitative action of cAMP.

Here we have demonstrated how cAMP signalling facilitates Th1 differentiation, and shown that $PGE_2$-EP4 signalling is representative of such cAMP signalling operating in T cells. Figure 8 depicts our model for cAMP-mediated Th1 differentiation and its cross-talk with PI3K pathway in TCR activation. In addition to prostanoids, there are a number of other agents that can activate cAMP signalling in T cells, such as catecholamines, histamine and adenosine[8]. Our results suggest a possibility that these substances similarly facilitate Th1 differentiation and promote immune inflammation. This is particularly the case for those substances that activates both PI3K and cAMP signalling simultaneously. Given that most of these receptors are G-protein coupled receptors (GPCRs), our present results show how GPCR signalling cooperates with cytokine signalling, that is, amplifying the latter actions by inducing their receptors. We propose to designate such GPCR actions as cytokine amplification and ligands of such GPCR as cytokine amplifiers. This cytokine amplifying action of GPCR ligands surely accounts for some of their pathophysiological actions and may, therefore, be of therapeutic consideration.

## Methods

**Mice.** C57BL/6 mice were obtained from Japan SLC (Shizuoka, Japan). EP2- and EP4-deficient and littermate control WT mice have been previously described[9]. Mice defective in IFN-γR1 on a C57BL/6 background[30] were kind gifts from M. Aguet. To generate EP4-deficient T cells, Lck-Cre mice[37] were crossed to lox-flanked *Ptger4* mice[38]. $SIK2^{-/-}$ mice have been described elsewhere[22] and were housed in the National Institute of Biomedical Innovation. All mice, except the $SIK2^{-/-}$ mice, were housed at the Institute of Laboratory Animals of Kyoto University on a 12-h light/dark cycle under specific pathogen-free conditions. All experimental procedures were approved by the Committee on Animal Research of Kyoto University Faculty of Medicine and National Institute of Biomedical Innovation.

**Plasmids.** WT CREB and the CREB(S133A) mutant plasmids were kindly provided by H. Bito. pGFP-mSIK2, pGFP-mSIK2 S587A, pGFP-mCRTC2 S171A and GAL4 fused pM-mCRTC2 and pTAL-5x GAL4 have been described[16,34].

**Reagents.** $PGE_2$ (100 nM) was obtained from Cayman Chemical. Agonists selective to each EP subtype (ONO-DI-004, ONO-AE1-259, ONO-AE-248 and ONO-AE1-329 for EP1, EP2, EP3 and EP4, respectively, each 100 nM) were kind gifts of Ono Pharmaceutical Co., Japan. Dibutyryl cAMP (db-cAMP, 100 μM), $N^6$-Bnz-cAMP (30–300 μM), wortmannin (100 nM), LY-294002 (1 μM), H-89 (10 μM), Rp-8-CPT-cAMPS (300 μM), Rp-8-Br-cAMPS (300 μM), Forskolin (1 μM) and 3-isobutyl-1-methylxanthine (100 μM) were purchased from Sigma. Cycloheximide (10 μM) and STS (5–50 nM) were purchased from Calbiochem.

**Preparation and culture of $CD4^+$ T cells.** Naive $CD4^+CD45RB^+CD25^-$ and $CD4^+$ T cells were purified from spleens and LNs by using FACS Aria2 (Becton Dickinson) and auto-MACS (Miltenyi), respectively. Cells were cultured in complete RPMI1640 medium containing 10% FBS. For *in vitro* activation of T cells, plate-bound antibodies to CD3 (10 μg ml$^{-1}$, clone 145-2C11, eBioscience) and CD28 (10 μg ml$^{-1}$ or indicated concentrations, clone 37.51, eBioscience) were used. For $T_H1$ differentiation, cells were stimulated with anti-CD3 and anti-CD28 for the first 2 days, and then without anti-CD3 and anti-CD28 antibodies for

another 24 h. Cells were cultured with 2,500 U ml$^{-1}$ rmIL-2, 10 ng ml$^{-1}$ rmIL-12 (R&D Systems) and 5 μg ml$^{-1}$ anti-IL-4 (clone 11B11, eBioscience) for 3 days. To reduce the background of phosphorylated CREB, freshly isolated CD4$^+$ T cells were cultured for 2 days in RPMI1640 medium and IL-7 (10 ng ml$^{-1}$, R&D Systems) that was added to maintain the survival of naive T cells[47]. In some culture conditions, 10 ng ml$^{-1}$ of IFN-γ (R&D Systems) or 10 μg ml$^{-1}$ of anti-mouse IFN-γ (clone XMG1.2, eBioscience), anti-mouse IL-12/IL-23 p40 (clone C17.8, eBioscience) or anti-mouse IL-2 (clone JES6-1A12, eBioscience) were added.

**Surface and intracellular staining.** For surface staining, CD4$^+$ T cells were directly stained with phycoerythrin (PE)-conjugated anti-mouse CD119 (IFN-γR1, clone 2E2, eBioscience), PE-conjugated rat anti-mouse CD122 (IL-2Rβ, clone TM-β1, BD Pharmingen) or PE-conjugated anti-mouse CD69 (clone H1.2F3, eBioscience), or stained firstly with hamster anti-mouse IL-12Rβ2 (BD Pharmingen) and then with PE-conjugated mouse anti-Armenian and Syrian hamster IgG cocktail (BD Pharmingen). For intracellular staining, CD4$^+$ T cells were restimulated with 50 ng ml$^{-1}$ PMA (Sigma) and 500 ng ml$^{-1}$ ionomycin (Sigma) in the presence of GolgiPlug (BD Pharmingen) for the last 4–5 h of incubation. Cells were fixed and permeabilized with Cytofix/Cytoperm (BD Pharmingen) and stained with fluorescein isothiocyanate (FITC)-conjugated antibody to IFN-γ (clone XMG1.2, eBioscience), and PE-conjugated antibody to IL-4 (clone 11B11, eBioscience). Quantitative flow cytometry was performed on an Epics XL-MCL (Beckman Coulter) or FACS Calibur (BD Bioscience).

**Fractionation and western blot.** Cytoplasmic and nuclear cell fractions were prepared using ProteoExtract Subcellular Proteome Extraction kit (Calbiochem). Western blotting was performed according to a protocol from Cell Signaling. Anti-mouse CREB, p-CREB (S133), STAT1, and p-STAT1 (Y701) antibodies were obtained from Cell Signaling. Anti-mouse GAPDH (6C5, Ambion), anti-mouse α-tubulin (DM 1A, Sigma) and anti-goat lamin B (C-20, Santa Cruz) were used as internal control. Anti-rabbit CRTC2 anti-serum has been described[20]. Immunoreactive proteins were visualized by using the enhanced chemiluminescence system from Fuji Film (LAS-3000).

**Enzyme-linked immunosorbent assay.** For the detection of IL-2 and IFNγ production, the supernatants of cell cultures were collected, and the manufacturer's instructions were followed (Pierce).

**Real-time PCR.** RNA purification and reverse transcription were performed by using Rneasy Mini Kit (Qiagen) and High-capacity cDNA Reverse Transcription Kits (ABI), respectively. Samples were analysed by real-time PCR with FastStart DNA Master$^{PLUS}$ SYBR Green I kit or LightCycler Taqman Master kit with Universal ProbeLibrary Set, Mouse (Roche). Primers and probes used in this study are listed in Supplementary Table S1. Expression was normalized to that of mouse 18S ribosomal RNA (*Rn18s*) or glyceraldehyde-3-phosphate dehydrogenase (*Gapdh*) gene and calculated relative to expression in vehicle control by the $2^{-\Delta\Delta Ct}$ method in each experiment.

**Microarray assay.** mRNA was converted to biotinylated antisense RNA using GeneChip HT 3′IVT Express Kit (Affymetrix) and biological duplicates were hybridized to Affymetrix GenChip Mouse Genome 430 2.0 Arrays (Affymetrix). Data were scaled, normalized by GeneChip Operating Software 1.4. After filtration, expression levels of selected probes were shown in bar graphs by using mean intensity of biological duplicates. Microarray data were deposited in GEO Data Sets under accession number GSE39592.

**Chromatin immunoprecipitation.** Freshly isolated WT CD4$^+$ T cells were cultured for 2 days in the presence of IL-7 followed by stimulation with db-cAMP (100 μM) or vehicle for another 1 h. Cells were crosslinked with 1% (vol/vol) formaldehyde and chromatin DNA was purified and digested by using SimpleChIP Enzymatic Chromatin IP Kits (Cell signaling) according to the manufacturer's instructions. Anti-p-CREB Ser133 antibody (Cell Signaling) and anti-CRTC2 antisera were used for immunoprecipitation. Precipitated DNA was quantified by real-time PCR (primer sets in Supplementary Tables S2 and S3) and was calculated relative to input DNA.

**RNAi and nucleofection.** Mouse *Creb1*, *Crtc2* and scrambled control siRNA were obtained from Stealth RNAi (Invitrogen). The sequence of Creb1 siRNA: 5′-UUGAACAACAACUUGGUUGCUGGGC-3′ (sense) or 5′-GCCCAGCAACC AAGUUGUUGUUCAA-3′ (antisense); Crtc2 siRNA: 5′-GCCAUGGCUCAGGA CCUAAUAUCAU-3′ (sense) or 5′-AUGAUAUUAGGUCCUGAGCCAUGGC-3′ (antisense). Freshly isolated CD4$^+$ T cells were transfected with 500 pmol siRNA using Amaxa P3 Primary Cell 4D-Nucleofector X Kit with the programme DN100 on a 4D-Nucleofector (Lonza) in 100 μl. Cells were directly transferred into full RPMI1640, then were cultured and stimulated in the presence of IL-7. Alternatively, CD4$^+$ T cells were preactivated with anti-CD3 and anti-CD28 for 2 days, then 'rest' on ice for 1–2 h followed by transfecting with 5 μg plasmids in 100 μl using Amaxa P3 Primary Cell 4D-Nucleofector X Kit with the programme EO115 on a 4D-Nucleofector (Lonza). Cells were then cultured and stimulated.

**Luciferase assay.** To determine the CRTC2 transcriptional activity, preactivated CD4$^+$ T cells were nucleofected with GAL4-fusion pM-mCRTC2 and pTAL-5x GAL4-Luciferase reporter and pRL-TK renilla luciferase reporte as internal control and treated with db-cAMP as indicated. To construct the mouse *Il12rb2* reporter vector, a 5′-upstream fragment from −4.4 kb to +70 bp of the mouse *Il12rb2* promoter/enhancer region were cloned by PCR and inserted into the pGL4.17 luciferase reporter vector (Promega). The sequence of primers: 5′-CTATGCTG CTGCCTGAAAGATGAGG-3′ (forward) and 5′-AGGGCACCTACCACTAT CCTCATCC-3′ (reverse). EL4 cells stably expressing the mouse *Il12rb2* reporter and the internal control renilla luciferase (Promega), EL4-*Il12rb2*-luc cells, were stimulated with anti-CD3 (5 μg ml$^{-1}$) and db-cAMP or vehicle for 24 h, then harvested for luciferase assay. Alternatively, EL4-*Il12rb2*-luc cells were transfected with siRNA or plasmids followed by stimulation with anti-CD3 and db-cAMP as described in the figure legend. Luciferase activities in cell lysates were detected by The Dual-Luciferase Reporter Assay System (Promega).

**CHS model.** We sensitized Lck-Cre$^-$EP4$^{fl/fl}$ and Lck-Cre$^+$EP4$^{fl/fl}$ mice with 25 μl of 1% (w/v) DNFB in acetone/olive oil (4/1, v/v) on shaved abdominal skin on day 0. dLN cells of one mouse were collected on day 5, and then transferred into one naive B6 mouse. The recipient mice were immediately challenged by application of 20 μl of 0.3 or 0.5% DNFB to their ear, and ear thickness was measured with a micrometre for each mouse before and 24 h after elicitation, and the difference is expressed as ear swelling. Alternatively, the dLN cells were harvested from DNFB-sensitized mice on day 5 to detect mRNA or protein expression of cytokine receptors or were subjected to isolation of CD4$^+$ T cells by antoMACS, and *in vitro* restimulated with anti-CD3 and anti-CD28 for 24 h for measuring cytokine production.

**Colitis model.** Adoptive transfer colitis model has been described[43]. Briefly, naive CD4$^+$CD25$^-$CD45RB$^{hi}$ T cells were prepared from Lck-Cre$^+$EP4$^{+/+}$ or Lck-Cre$^+$EP4$^{flox/+}$ mice by cell sorting. Cells ($5 \times 10^5$ cells per mouse) were transferred intravenously into mice deficient in recombination-activating gene 2 (*Rag2*). CD4$^+$ T cells from mesenteric lymph nodes of each recipient mouse were purified by auto-MACS on day 42 after T-cell transfer and stimulated with anti-CD3 for 72 h. IFN-γ and IL-2 production in supernatants and gene expression in CD4$^+$ T cells were determined by enzyme-linked immunosorbent assay and real-time PCR, respectively.

**Data analysis.** All data were expressed as mean ± s.e.m., and statistical significance was examined by the unpaired two-tail Student's *t*-test except where indicated, using GraphPad (Prism) or Excel (Microsoft).

## References


1. Zhu, J. & Paul, W. E. CD4 T cells: fates, functions, and faults. *Blood* **112,** 1557–1569 (2008).
2. Liao, W., Lin, J., Wang, L., Li, P. & Leonard, W. J. Modulation of cytokine receptors by IL-2 broadly regulates differentiation into helper T cell lineages. *Nat. Immunol.* **12,** 551–559 (2011).
3. Smith-Garvin, J. E., Koretzky, G. A. & Jordan, M. S. T Cell Activation. *Annu. Rev. Immunol.* **27,** 591–619 (2009).
4. Bourne, H. R. *et al.* Modulation of inflammation and immunity by cyclic AMP. *Science* **184,** 19–28 (1974).
5. Kammer, G. M. The adenylate cyclase-cAMP-protein kinase A pathway and regulation of the immune response. *Immunol. Today* **9,** 222–229 (1988).
6. Betz, M. & Fox, B. S. Prostaglandin $E_2$ inhibits production of Th1 lymphokines but not of Th2 lymphokines. *J. Immunol.* **146,** 108–113 (1991).
7. Moore, A. R. & Willoughby, D. A. The role of cAMP regulation in controlling inflammation. *Clin. Exp. Immunol.* **101,** 387–389 (1995).
8. Mosenden, R. & Tasken, K. Cyclic AMP-mediated immune regulation – overview of mechanisms of action in T cells. *Cell Signal* **23,** 1009–1016 (2011).
9. Yao, C. *et al.* Prostaglandin $E_2$-EP4 signaling promotes immune inflammation through $T_H1$ cell differentiation and $T_H17$ cell expansion. *Nat. Med.* **15,** 633–640 (2009).
10. Chen, Q. *et al.* A novel antagonist of the prostaglandin $E_2$ $EP_4$ receptor inhibits Th1 differentiation and Th17 expansion and is orally active in arthritis models. *Br. J. Pharmacol.* **160,** 292–310 (2010).
11. Nataraj, C. *et al.* Receptors for prostaglandin $E_2$ that regulate cellular immune responses in the mouse. *J. Clin. Invest.* **108,** 1229–1235 (2001).
12. Libioulle, C. *et al.* Novel Crohn disease locus identified by genome-wide association maps to a gene desert on 5p13.1 and modulates expression of *PTGER4*. *PLoS Genet.* **3,** e58 (2007).
13. Khor, B., Gardet, A. & Xavier, R. J. Genetics and pathogenesis of inflammatory bowel disease. *Nature* **474,** 307–317 (2011).

14. The International Multiple Sclerosis Genetics Consortium & the Wellcome Trust Case Control Consortium. Genetic risk and a primary role for cell-mediated immune mechanisms in multiple sclerosis. *Nature* **476,** 214–219 (2011).
15. Bossini-Castillo, L. *et al.* A GWAS follow-up study reveals the association of the IL12RB2 gene with systemic sclerosis in Caucasian populations. *Hum. Mol. Genet.* **21,** 926–933 (2012).
16. Li, X. *et al.* Divergent requirement for Gαs and cAMP in the differentiation and inflammatory profile of distinct mouse Th subsets. *J. Clin. Invest.* **122,** 963–973 (2012).
17. Mayr, B. & Montminy, M. Transcriptional regulation by the phosphorylation-dependent factor CREB. *Nat. Rev. Mol. Cell. Biol.* **2,** 599–609 (2001).
18. Altarejos, J. Y. & Montminy, M. CREB and the CRTC-co-activators: sensors for hormonal and metabolic signals. *Nat. Rev. Mol. Cell. Biol.* **12,** 141–151 (2011).
19. Sasaki, T. *et al.* SIK2 is a key regulator for neuronal survival after ischemia via TORC1-CREB. *Neuron* **69,** 106–119 (2011).
20. Katoh, Y. *et al.* Silencing the constitutive active transcription factor CREB by the LKB1-SIK signaling cascade. *FEBS J.* **273,** 2730–2748 (2006).
21. Screaton, R. A. *et al.* The CREB coactivator TORC2 functions as a calcium- and cAMP-sensitive coincidence detector. *Cell* **119,** 61–74 (2004).
22. Horike, N. *et al.* Down-regulation of SIK2 expression promotes the melanogenic program in mice. *Pigment Cell. Melanoma Res.* **23,** 809–819 (2010).
23. Szabo, S. J., Dighe, A. S., Gubler, U. & Murphy, K. M. Regulation of the interleukin (IL)-12R β2 subunit expression in developing T helper 1 (Th1) and Th2 cells. *J. Exp. Med.* **185,** 817–824 (1997).
24. Afkarian, M. *et al.* T-bet is a STAT1-induced regulator of IL-12R expression in naïve $CD4^+$ T cells. *Nat. Immunol.* **3,** 549–508 (2002).
25. Watford, W. T. *et al.* Signaling by IL-12 and IL-23 and the immunoregulatory roles of STAT4. *Immunol. Rev.* **202,** 139–156 (2004).
26. Skrenta, H., Yang, Y., Pestka, S. & Fathman, C. G. Ligand-independent down-regulation of ifn-γ receptor 1 following tcr engagement. *J. Immunol.* **164,** 3506–3511 (2000).
27. Schulz, E. G., Mariani, L., Radbruch, A. & Hofer, T. Sequential polarization and imprinting of type 1 T helper lymphocytes by interferon-g and interleukin-12. *Immunity* **30,** 673–683 (2009).
28. Hirata, K. & Narumiya, S. Prostanoid Receptors. *Chem. Rev.* **111,** 6209–6230 (2011).
29. Chang, J. T., Shevach, E. M. & Segal, B. M. Regulation of interleukin (IL)-12 receptor β2 subunit expression by endogenous IL-12: a critical step in the differentiation of pathogenic autoreactive T cells. *J. Exp. Med.* **189,** 969–978 (1999).
30. Huang, S. *et al.* Immune response in mice that lack the interferon-γ receptor. *Science* **259,** 1742–1745 (1993).
31. Kane, L. P., Andres, P. G., Howland, K. C., Abbas, A. K. & Weiss, A. Akt provides CD28 costimulatory signal for up-regulation of IL-2 and IFN-γ but not $T_H2$ cytokines. *Nat. Immunol.* **2,** 37–44 (2001).
32. Murray, A. J. Pharmacological PKA inhibition: all may not be what it seems. *Sci. Signal.* **1,** re4 (2008).
33. Bjorgo, E. *et al.* Cross talk between phosphatidylinositol 3-kinase and cyclic AMP (cAMP)-protein kinase a signaling pathways at the level of a protein kinase B/beta-arrestin/cAMP phosphodiesterase 4 complex. *Mol. Cell. Biol.* **30,** 1660–1672 (2010).
34. Christensen, A. E. *et al.* cAMP analog mapping of Epac1 and cAMP kinase. Discriminating analogs demonstrate that Epac and cAMP kinase act synergistically to promote PC-12 cell neurite extension. *J. Biol. Chem.* **278,** 35394–35402 (2003).
35. Ravnskjaer, K. *et al.* Cooperative interactions between CBP and TORC2 confer selectivity to CREB target gene expression. *EMBO J.* **26,** 2880–2889 (2007).
36. Muraoka, M. *et al.* Involvement of SIK2/TORC2 signaling cascade in the regulation of insulin-induced PGC-1alpha and UCP-1 gene expression in brown adipocytes. *Am. J. Physiol. Endocrinol. Metab.* **296,** E1430–E1439 (2009).
37. Takahama, Y. *et al.* Functional competence of T cells in the absence of glycosylphosphatidylinositol-anchored proteins caused by T cell-specific disruption of the *Pig-a* gene. *Eur. J. Immunol.* **28,** 2159–2166 (1998).
38. Schneider, A. *et al.* Generation of a conditional allele of the mouse prostaglandin EP4 receptor. *Genesis* **40,** 7–14 (2004).
39. Nakajima, S. *et al.* Prostaglandin $I_2$-IP signaling promotes Th1 differentiation in a mouse model of contact hypersensitivity. *J. Immunol.* **184,** 5595–5603 (2010).
40. Vang, T. *et al.* Activation of the Cooh-Terminal Src Kinase (Csk) by camp-dependent protein kinase inhibits signaling through the T cell receptor. *J. Exp. Med.* **193,** 497–508 (2001).
41. Wang, B. *et al.* $CD4^+$ Th1 and $CD8^+$ Type 1 cytotoxic T cells both play a crucial role in the full development of contact hypersensitivity. *J. Immunol.* **165,** 6783–6790 (2000).
42. Ostanin, D. V. *et al.* T cell transfer model of chronic colitis: concepts, considerations, and tricks of the trade. *Am. J. Physiol. Gastrointest. Liver Physiol.* **296,** G135–G146 (2009).
43. Stallmach, A. *et al.* Increased expression of interleukin-12 receptor β2 on lamina propria mononuclear cells of patients with active Crohn's disease. *Int. J. Colorectal. Dis.* **17,** 303–310 (2002).
44. Kirman, I., Nielsen, O. H., Kjaersgaard, E. & Brynskov, J. Interleukin-2 receptor alpha and beta chain expression by circulating alpha beta and gamma delta T cells in inflammatory bowel disease. *Dig. Dis. Sci.* **40,** 291–295 (1995).
45. Ochaion, A. *et al.* The anti-inflammatory target A3 adenosine receptor is over-expressed in rheumatoid arthritis, psoriasis and Crohn's disease. *Cell Immunol.* **258,** 115–122 (2009).
46. Esaki, Y. *et al.* Dual roles of $PGE_2$-EP4 signaling in mouse experimental autoimmune encephalomyelitis. *Proc. Natl. Acad. Sci. USA* **107,** 12233–12238 (2010).
47. Rathmell, J. C., Farkash, E. A., Gao, W. & Thompson, C. B. IL-7 enhances the survival and maintains the size of naive T cells. *J. Immunol.* **167,** 6869–6876 (2001).

## Acknowledgements

We thank Ono Pharmaceutical Co. (Osaka, Japan) for supplying EP agonists, Protein-Express Co., Ltd. (Chiba, Japan) for permission to use SIK2-deficient mice, and Centre for Innovation in Immunoregulative Technology and Therapeutics of Kyoto University for supporting cell sorting. We also thank T. Taniguchi, M. Aguet, M. Hikida, Y. Takahama, M.D. Breyer and R.M. Breyer for gene-targeted mice, H. Bito for plasmids-harbouring CREB WT and S133A mutant, M. Mizutani for animal care, A. Ehrlich for reviewing English in our manuscript, D. Sakata, K. Nonomura, T. Aoki, A. Nomachi, A. Washimi and T. Arai for assistance. This work is supported by Grants-in-Aid for Scientific Research from the Ministry of Education, Culture, Sports, Science and Technology of Japan, a grant from CREST of JST, and a grant from Health Labour Sciences Research Grant. C.Y. was supported by the Japan Society for the Promotion of Science (JSPS).

## Author contributions

C.Y. and S.N. designed the experiments. C.Y. did all experiments with assistance from K.S. for CHS, X.M. for colitis, and T.H. for cell sorting and colitis. H.T. provided SIK2KO mice, CRTC2 antisera and plasmids-expressing WT, and mutant mSIK2 and mCRTC2, and contributed to discussion. C.Y., T.H. and S.N. performed data analysis. S.N. supervised the project. C.Y. and S.N. wrote the manuscript.

## Additional information

**Supplementary Information** accompanies this paper on http://www.nature.com/naturecommunications

**Competing financial interests:** The authors declare no competing financial interests.

**Reprints and permission** information is available online at http://npg.nature.com/reprintsandpermissions/

**How to cite this article:** Yao, C. *et al.* Prostaglandin $E_2$ promotes Th1 differentiation via synergistic amplification of IL-12 signalling by cAMP and PI3-Kinase. *Nat. Commun.* 4:1685 doi: 10.1038/ncomm2684 (2013).

Stem Cell Reports
Resource
ISSCR
OPEN ACCESS

# Long-Term Self-Renewal of Human ES/iPS-Derived Hepatoblast-like Cells on Human Laminin 111-Coated Dishes

Kazuo Takayama,[1,2,3] Yasuhito Nagamoto,[1,2] Natsumi Mimura,[2] Katsuhisa Tashiro,[4] Fuminori Sakurai,[1] Masashi Tachibana,[1] Takao Hayakawa,[5] Kenji Kawabata,[4] and Hiroyuki Mizuguchi[1,2,3,6,*]
[1]Laboratory of Biochemistry and Molecular Biology, Graduate School of Pharmaceutical Sciences, Osaka University, Osaka 565-0871, Japan
[2]Laboratory of Hepatocyte Differentiation, National Institute of Biomedical Innovation, Osaka 567-0085, Japan
[3]iPS Cell-Based Research Project on Hepatic Toxicity and Metabolism, Graduate School of Pharmaceutical Sciences, Osaka University, Osaka 565-0871, Japan
[4]Laboratory of Stem Cell Regulation, National Institute of Biomedical Innovation, Osaka 567-0085, Japan
[5]Pharmaceutical Research and Technology Institute, Kinki University, Osaka 577-8502, Japan
[6]The Center for Advanced Medical Engineering and Informatics, Osaka University, Osaka 565-0871, Japan
*Correspondence: mizuguch@phs.osaka-u.ac.jp
http://dx.doi.org/10.1016/j.stemcr.2013.08.006


## SUMMARY

The establishment of self-renewing hepatoblast-like cells (HBCs) from human pluripotent stem cells (PSCs) would realize a stable supply of hepatocyte-like cells for medical applications. However, the functional characterization of human PSC-derived HBCs was not enough. To purify and expand human PSC-derived HBCs, human PSC-derived HBCs were cultured on dishes coated with various types of human recombinant laminins (LN). Human PSC-derived HBCs attached to human laminin-111 (LN111)-coated dish via integrin alpha 6 and beta 1 and were purified and expanded by culturing on the LN111-coated dish, but not by culturing on dishes coated with other laminin isoforms. By culturing on the LN111-coated dish, human PSC-derived HBCs were maintained for more than 3 months and had the ability to differentiate into both hepatocyte-like cells and cholangiocyte-like cells. These expandable human PSC-derived HBCs would be manageable tools for drug screening, experimental platforms to elucidate mechanisms of hepatoblasts, and cell sources for hepatic regenerative therapy.

## INTRODUCTION

Human embryonic stem cells (hESCs) and human induced pluripotent stem cells (hiPSCs) have the ability to self-replicate and to differentiate into all types of body cells including hepatoblasts and hepatocytes. Although cryopreserved primary human hepatocytes are useful in drug screening and liver cell transplantation, they rapidly lose their functions (such as drug metabolism capacity) and hardly proliferate in in vitro culture systems. On the other hand, human hepatic stem cells from fetal and postnatal human liver are able to self-replicate and able to differentiate into hepatocytes (Schmelzer et al., 2007; Zhang et al., 2008). However, the source of human hepatic stem cells is limited, and these cells are not available commercially. Therefore, the human pluripotent stem cell (hPSC)-derived hepatoblast-like cells (HBCs), which have potential to differentiate into the hepatocyte-like cells, would be an attractive cell source to provide abundant hepatocyte-like cells for drug screening and liver cell transplantation.

Because expandable and multipotent hepatoblasts or hepatic stem cells are of value, suitable culture conditions for the maintenance of hepatoblasts or hepatic stem cells obtained from fetal or adult mouse liver were developed (Kamiya et al., 2009; Tanimizu et al., 2004). Soluble factors, such as hepatocyte growth factor (HGF) and epidermal growth factor (EGF), are known to support the proliferation of mouse hepatic stem cells and hepatoblast (Kamiya et al., 2009; Tanimizu et al., 2004). Extracellular matrix (ECM) also affects the maintenance of hepatoblasts or hepatic stem cells. Laminin can maintain the character of mouse hepatoblasts (Dlk1-positive cells) (Tanimizu et al., 2004). However, the methodology for maintaining HBCs differentiated from hPSCs has not been well investigated. Zhao et al. (2009) have reported that hESC-derived hepatoblast-like cells (sorted N-cadherin-positive cells were used) could be maintained on STO feeder cells. Although a culture system using STO feeder cells for the maintenance of hepatoblast-like cells might be useful, there are two problems. The first problem is that N-cadherin is not a specific marker for human hepatoblasts. N-cadherin is also expressed in hESC-derived mesendoderm cells and definitive endoderm (DE) cells (Sumi et al., 2008). The second problem is that residual undifferentiated cells could be maintained on STO feeder cells. Therefore, their culture condition cannot rule out the possibility of the proliferation of residual undifferentiated cells. Because it is known that hPSC-derived cells have the potential to form teratomas in the host, the production of safer hepatocyte-like cells or hepatoblast-like cells has been required. Therefore, we decided to purify hPSC-derived HBCs, which can differentiate into mature hepatocyte-like cells, and then expand these cells.

In this study, we attempt to determine a suitable culture condition for the extensive expansion of HBCs derived

from hPSCs. We found that the HBCs derived from hPSCs can be maintained and proliferated on human laminin-111 (LN111)-coated dishes. To demonstrate that expandable, multipotent, and safe (i.e., devoid of residual undifferentiated cells) hPSC-derived HBCs could be maintained under our culture condition, the hPSC-derived HBCs were used for hepatic and biliary differentiation, colony assay, and transplantation into immunodeficient mice.

## RESULTS

### Human PSC-Derived Hepatoblast-like Cells Could Adhere onto Human LN111 via Integrin α6 and β1

The HBCs were generated from hPSCs (hESCs and hiPSCs) as described in Figure 1A (details of the characterization of hPSC-derived HBCs are described in Figure 3). Definitive endoderm differentiation of hPSCs was promoted by stage-specific transient transduction of FOXA2 in addition to the treatment with appropriate soluble factors (such as Activin A). Overexpression of FOXA2 is not necessary for establishing the hPSC-derived HBCs, but it is helpful for efficient generation of the hPSC-derived HBCs. On day 9, these hESC-derived populations contained two cell populations with distinct morphology (Figure 1B). One population resembled human hepatic stem cells that were isolated from human fetal liver (shown in red) (Schmelzer et al., 2007), whereas the other population resembled definitive endoderm cells (shown in green) (Hay et al., 2008). The population that resembled human hepatic stem cells was alpha-1-fetoprotein (AFP) positive, whereas the other population was AFP negative (Figure 1C, left). On day 9, the percentage of AFP-positive cells was approximately 80% (Figure 1C, right). To characterize these two cell populations (hESC-derived HBC and non-HBC [NHBC] populations), the colonies were manually isolated by using a pipette, and then the gene expression analysis was performed. The gene expression levels of *AFP*, *CD133*, *EpCAM*, *CK8*, and *CK18* in the hESC-derived HBCs were higher than those in the bulk population containing both hESC-derived HBCs and NHBCs (*CD133*, *EpCAM*, *CK8*, and *CK18* were named as pan-hepatoblast markers and are known to be strongly expressed in both human hepatic stem cells and hepatoblasts [Schmelzer et al., 2007; Zhang et al., 2008]) (Figure 1D). On the other hand, the gene expressions of *AFP*, *CD133*, *EpCAM*, *CK8*, and *CK18* in the hESC-derived NHBCs were hardly detected. The gene expression levels of DE, mesendoderm, and pluripotent markers in the hESC-derived NHBCs were higher than those in the hESC-derived HBCs, indicating that the hESC-derived NHBCs could remain in a more undifferentiated state than the hESC-derived HBCs (Figures S1A–S1C available online). These results suggest that hepatoblast-like cells could be differentiated from hPSCs.

To purify the hESC-derived HBCs, these cells were plated onto dishes coated with various laminins. There are 15 different laminin isoforms in human tissues. Although laminin is known to be useful to sustain mouse hepatoblasts (Tanimizu et al., 2004), it remains unknown which human laminin isoform has the potential to purify and expand the HBCs. To identify a human laminin isoform that would be useful for purifying hESC-HBCs, the hESC-HBCs and -NHBCs were plated onto dishes coated with various types of commercially available human laminins (Figure 1E). The hESC-derived HBCs could more efficiently adhere onto the human LN111-coated dish compared with hESC-derived NHBCs or unseparated populations (containing both HBCs and NBCs). These data suggest that a hESC-derived HBC population can be purified from the unseparated populations by culturing on human LN111-coated dishes. Because integrins are known to be important molecules for cell adhesion to the ECM including laminins, we expected that certain types of integrins would allow selective adhesion of the hESC-derived HBCs to human LN111-coated dish. The gene expression levels of various integrins were examined (Figure 1F). Among the integrin α subunits, the gene expression level of *integrin α6* in the hESC-derived HBCs was significantly higher than that in the hESC-derived NHBCs. In contrast, among the integrin β subunits, the gene expression level of *integrin β1* was higher than those of *integrin β2* and *β3* in all cell populations. The hESC-derived HBCs, but not NHBCs, expressed both integrin α6 and β1 (Figure S1D). Almost all adhesion of the hESC-derived HBCs to a human LN111-coated dish was inhibited by both function-blocking antibodies to integrin α6 and β1 (Figure 1G). These results indicated that the hESC-derived HBCs could attach to a human LN111-coated dish via integrin α6 and β1.

### The hPSC-Derived HBCs Could Be Proliferated and Maintained on a Human LN111-Coated Dish

To obtain the purified hESC-derived HBC population, the hESC-derived cells (day 9) were plated onto a human LN111-coated dish, and then unattached cells were removed at 15 min after plating (Figure 2A). Among various laminins, only human LN111 could proliferate (Figure 2B) and purify (Figure 2C) the AFP-positive population in the presence of HGF and EGF. During culture on the human LN111-coated dish, the morphology of the hESC-derived HBCs gradually changed into that of human hepatoblasts (Figure S1E) (Schmelzer et al., 2007). Therefore, the characteristics of hESC-derived HBCs might be changed by culturing on a human LN111-coated dish (details of the characterization of the hESC-derived HBCs are described in Figure 3). After culturing on a human LN111-coated

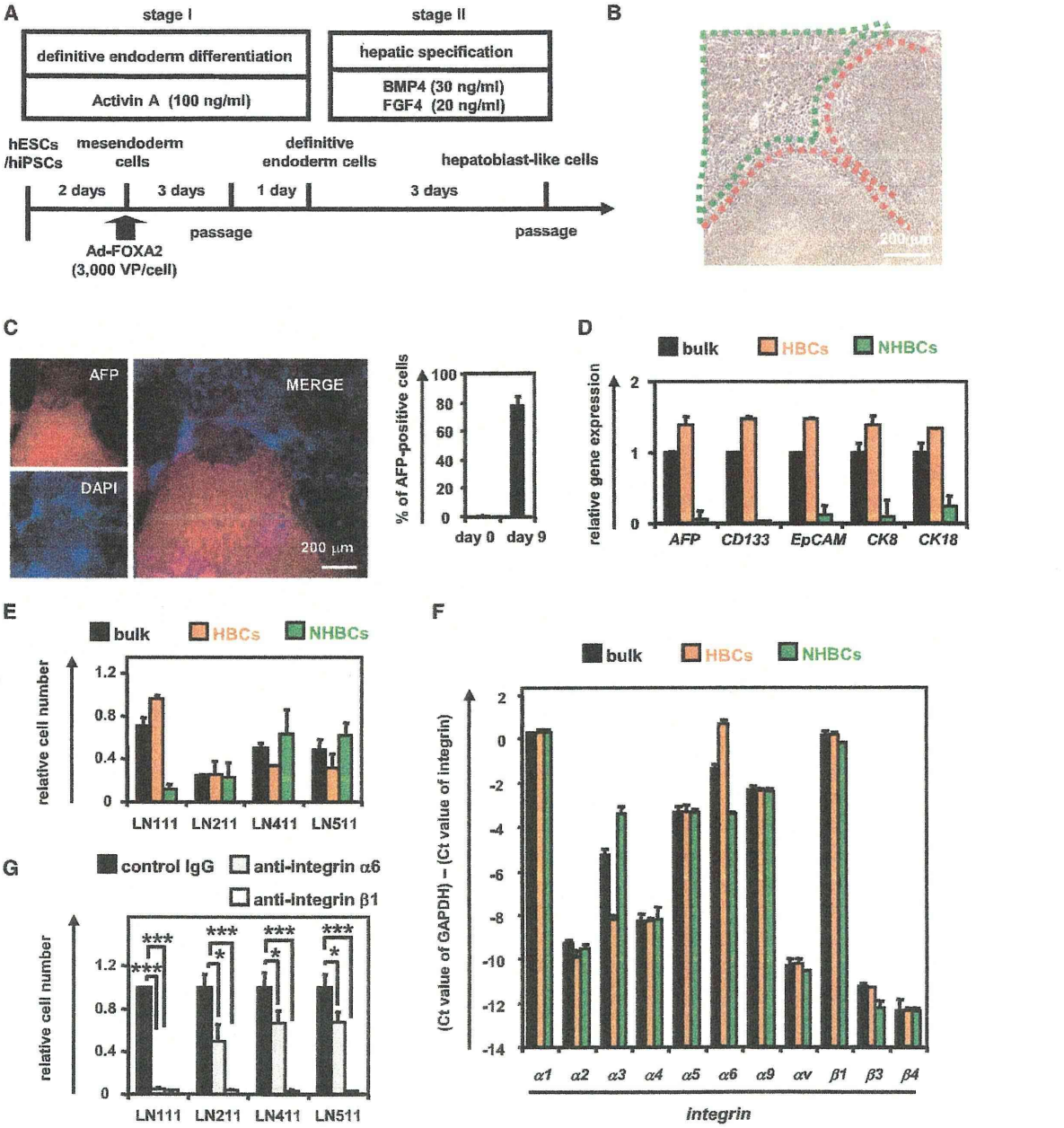


**Figure 1. The Human ESC-Derived HBCs Selectively Attached to a Human LN111-Coated Dish via Integrin α6 and β1**

(A) The procedure for the differentiation of hESCs (H9) into hepatoblast-like cells (HBCs) is presented schematically. Details are described in the Experimental Procedures.

(B) Phase-contrast micrographs of the hESC-derived HBCs (red) and non-HBCs (NHBCs) (green) are shown.

(C) The hESC-derived cells (day 9) were subjected to immunostaining with anti-AFP (red) antibodies. The percentage of AFP-positive cells was examined on day 0 or 9 by using FACS analysis. Data represent the mean ± SD from ten independent experiments. Cells on "day 0" and "day 9" were compared using Student's t test ($p < 0.01$).

(D) On day 9, the hESC-derived HBCs and NHBCs were manually picked, and the gene expression levels of *AFP* and pan-hepatoblast markers (*CD133*, *EpCAM*, *CK8*, and *CK18*) were measured by real-time RT-PCR. The gene expression levels of *AFP* and pan-hepatoblast markers in the hESC-derived cells (day 9; bulk) were taken as 1.0. Data represent the mean ± SD from four independent experiments. The gene expression levels in the HBCs were significantly different among the three groups (bulk, HBCs, and NHBCs) based on analysis with one-way ANOVA followed by Bonferroni post hoc tests ($p < 0.05$).

*(legend continued on next page)*

dish for a week, almost all of the cells were still AFP positive (Figures 2C and 2D). To characterize the cells cultured on various types of human laminins for 7 days, the gene expression levels of *AFP* and pan-hepatoblast (*CD133*, *CK8*, *CK18*, and *EpCAM*) markers were examined on day 16 (Figure 2E). The gene expression levels of *AFP* and pan-hepatoblast markers in the hESC-derived HBCs P1 (HBCs passaged once) did not change as compared with those of the hESC-derived HBCs (day 9; HBC P0) (the definitions of HBC P0, P1, P10, and clone in the present study are shown in Figure S3). The gene expression levels of mature hepatocyte and cholangiocyte markers in the hESC-derived HBC P1 did not change as compared with those of the hESC-derived HBC P0 (day 9) (Figure S1F). These results suggest that the characteristics of the hESC-derived HBC P1 are similar to those of the hESC-derived HBC P0, although their morphologies are quite different from each other. Interestingly, the gene expression levels of mature cholangiocyte markers in the cells cultured on human LN411- or 511-coated dishes were upregulated as compared with those of the hESC-derived HBC P0 (day 9) (Figure S1F), suggesting that human LN411 and 511 might promote biliary differentiation. Importantly, both hESC-derived HBCs and hiPSC-derived HBCs could extensively proliferate on a human LN111-coated dish for more than 15 passages (Figure 2F) in the presence of HGF and EGF. Doubling times of hESC (H9)-derived HBCs and hiPSC (Dotcom)-derived HBCs were approximately 78 and 67 hr, respectively. Almost all of the populations cultured on a human LN111-coated dish were AFP positive (Figure 2G). Taken together, these results suggested that the hPSC-derived HBCs would proliferate and be maintained on a human LN111-coated dish.

### Characterization of the hESC-Derived HBCs

To characterize the hESC-derived HBCs, the gene expression profiles in the hESC-derived purified HBCs (HBC P0), short-term cultured HBCs (HBCs passaged once [HBC P1]), and long-term cultured HBC (HBCs passaged ten times [HBC P10]) were examined. The hESC-derived HBCs were AFP positive (Figure 3A). Although the hESC-derived HBC P0 were negative for ALB, CK7, and CK19, the hESC-derived HBC P1 and P10 were positive for these genes (Figure 3A). Both integrin α6 and β1 (receptors of LN111) were strongly expressed in the hESC-derived HBC P0, P1, and P10 (Figure 3B). The gene expression levels of human hepatic stem cell markers (*N-CAM* and *Claudin 3* [Schmelzer et al., 2007]; these are not expressed in human hepatoblasts) in the hESC-derived HBC P0 were higher than those of the hESC-derived HBC P1 and P10 (Figure 3C). However, the gene expression level of *CK19* in the hESC-derived HBC P0 was lower than that of the hESC-derived HBC P1 and P10. The gene expression levels of pan-hepatoblast markers in the hESC-derived HBC P0 were similar to those of the hESC-derived HBC P1 and P10 (Figure 3D). The gene expression levels of human hepatoblast markers (*ALB*, *CYP3A7*, and *I-CAM* (Schmelzer et al., 2007), none of which were expressed in human hepatic stem cells) in the hESC-derived HBC P1 and P10 were higher than those of the hESC-derived HBC P0 (Figure 3E). However, the AFP expression level in the hESC-derived HBC P0 was similar to that of the hESC-derived HBC P1 and P10. Because the gene expression levels of mature hepatocyte and cholangiocyte markers in the hESC-derived HBC P1 and P10 were not increased as compared with those in the hESC-derived HBC P0 (Figure 3F), the hESC-derived HBC P1 and P10 were not segregated into either of the hepatic and biliary lineages. We also examined the gene expression levels of hepatoblast markers, which have been reported only in mice and not in humans (Figure 3G). The characteristics of the hPSC-derived HBCs are summarized in Figure S3. In addition, hESC-derived HBC P0 and HBC P10 showed normal karyotypes (Figure S2A). Therefore, the genetic stability of the HBCs was confirmed throughout the maintenance period. Taken together, these results suggest that the hESC-derived HBC P0 resemble human hepatic stem cells and the hESC-derived HBC P1 and P10 resemble human hepatoblasts, although some gene expression patterns in the hESC-derived HBCs differ from those in human hepatic stem cells and human hepatoblasts, respectively.

(E) The hESC-derived cells (day 9; bulk), HBCs, and NHBCs were plated onto human LN111-, 211-, 411-, or 511-coated dishes, and the attached cells were counted at 60 min after plating. The cell number that was initially plated was taken as 1.0. Data represent the mean ± SD from four independent experiments. The number of attached HBCs on LN111-coated dishes were significantly different among three groups (bulk, HBCs, and NHBCs) based on analysis with one-way ANOVA followed by Bonferroni post hoc tests ($p < 0.05$).

(F) The gene expression levels of the indicated integrins were measured in the hESC-derived cells (day 9; bulk), HBCs, and NHBCs by real-time RT-PCR. Data represent the mean ± SD from four independent experiments. The gene expression levels of *integrin α3* and *α6* in the HBCs were significantly different among three groups (bulk, HBCs, and NHBCs) based on analysis with one-way ANOVA followed by Bonferroni post hoc tests ($p < 0.05$).

(G) The adhesion of the hESC-derived HBCs to human LN111-, 211-, 411-, or 511-coated dishes was examined by using the indicated integrin antibodies. IgG antibodies were used as a control for uninhibited cell adhesion. The number of attached cells was estimated at 60 min after plating. The cell number in the control IgG-treated group was taken as 1.0. Data represent the mean ± SD from three independent experiments. "Control IgG" and "anti-integrin α6 or integrin β1" were compared using Student's t test. $^{*}p < 0.05$; $^{***}p < 0.001$. See also Figure S1 and Tables S2–S5.

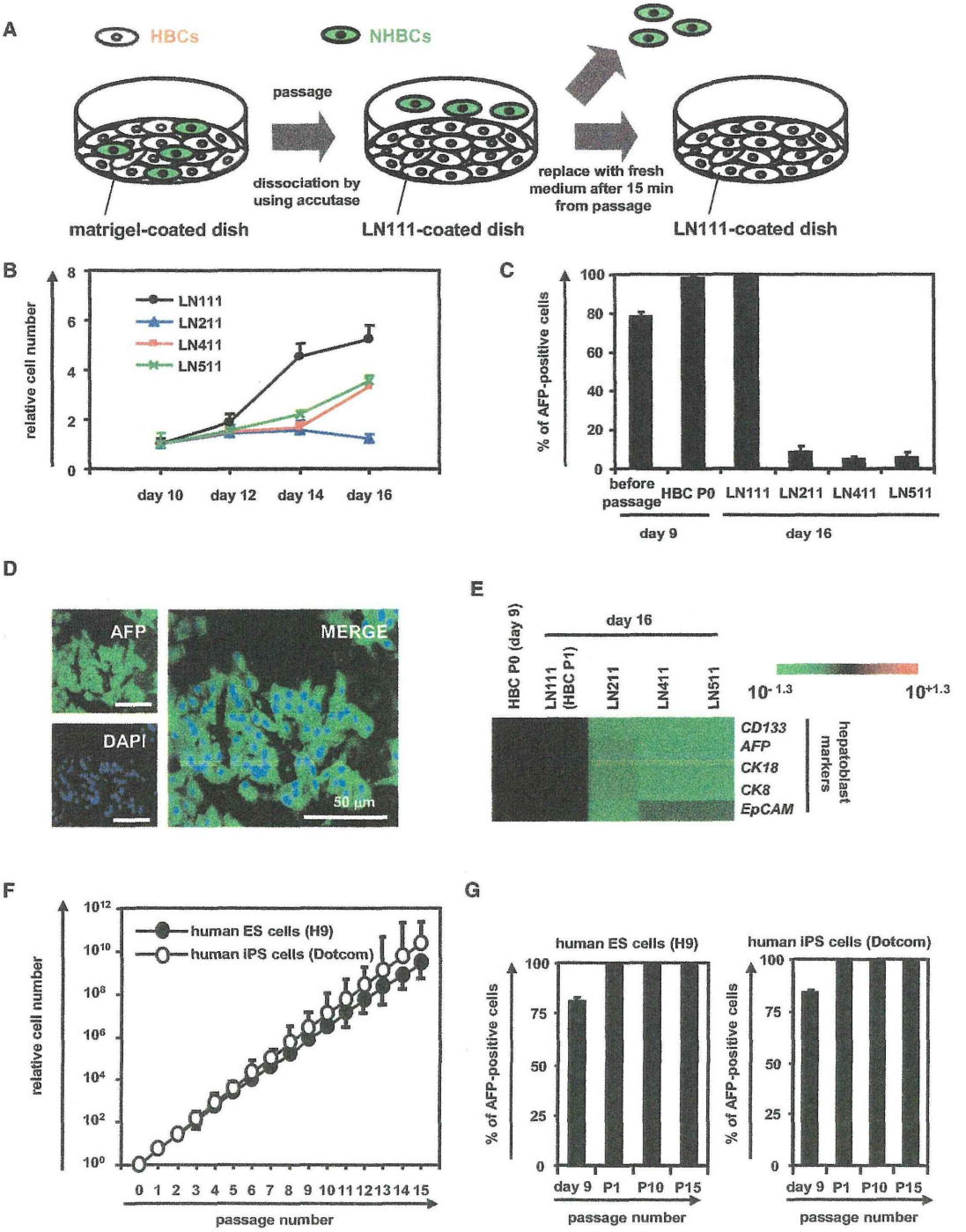


**Figure 2. The hESC-Derived HBCs Could Be Proliferated and Maintained on a Human LN111-Coated Dish**

(A) The hESC (H9)-derived cells (day 9) were plated onto a human LN111-coated dish. At 15 min after plating, the unattached cells were removed.

(B) The hESC (H9)-derived cells (day 9) were plated onto a human LN111, 211, 411, or 511-coated dish, and then the cell number were counted on days 10, 12, 14, and 16. The cell number on day 10 was taken as 1.0. Data represent the mean ± SD from three independent experiments. "LN111" was significantly different among four groups (LN111, 211, 411, and 511) on day 14 and 16 based on analysis with one-way ANOVA followed by Bonferroni post hoc tests ($p < 0.05$).

*(legend continued on next page)*

In order to examine whether the hESC-derived HBC P0 have the potential to proliferate clonally on various types of human laminins, single HBCs were plated on separate wells of a human LN111-coated 96-well plate at a low density (one cell per one well) (Table S1). Single cells that attached to the human LN111-coated dish were AFP positive and HNF4α positive (Figure S2B). At 7 days after plating, the hESC-derived HBC colonies (albumin [ALB]- and cytokeratin 7 [CK7] double positive) (a representative colony is shown in Figure S2C) were efficiently generated from the hESC-derived HBC P0 on a LN111-coated dish. Taken together, these results showed that the hESC-derived HBCs could be generated from both the hESC-derived HBC P0 population and the single hESC-derived HBC P0.

### The hPSC-Derived HBCs Could Differentiate into Both Hepatic and Biliary Lineages In Vitro

To examine whether the hESC-derived HBCs have the potential to differentiate into both hepatic and biliary lineages, first, these cells were differentiated into hepatocyte-like cells as described in Figure 4A. After 2 weeks of hepatic differentiation, almost all of the cells were polygonal in shape (Figure 4B) and were CYP3A4, αAT, and ALB positive (Figure 4C). The gene expression levels of mature hepatocyte markers in the HBC P0-, HBC P10-, or HBC clone-derived hepatocyte-like cells were higher than those in the cells that had not undergone hepatic differentiation (Figure 4D), although the gene expression levels of mature cholangiocyte markers in these cells did not change (Figure 4E). The ASGR1-positive cells in the HBC P0-, HBC P10-, and HBC clone-derived population accounted for approximately 60%, 90%, and 90% of the total, respectively (Figure 4F). The HBC P0-, HBC P10-, or HBC clone-derived hepatocyte-like cells had the ability to produce ALB (Figure 4G, left) and urea (Figure 4G, right). Next, the hESC-derived HBCs were differentiated into cholangiocyte-like cells as described in Figure 4H. After 2 weeks of biliary differentiation, tubular structures (Figure 4I) that were CK7 positive (Figure 4J) were observed. Although the gene expression levels of mature hepatocyte markers (Figure 4K) in the HBC P0-, HBC P10-, or HBC clone-derived cholangiocyte-like cells did not change, the gene expression levels of mature cholangiocyte markers (Figure 4L) in these cells were higher than those in the cells that had not undergone differentiation. Similar results were obtained by using another hESC line (H1) and hiPSC line (Dotcom) (Figure S4). Moreover, HBC-derived hepatocyte-like cells exhibited CYP metabolism capacity (Figure S5A) and a functional urea cycle that could response to ammonia (Figure S5B) and were considered to have potential to be applied in the prediction of drug-induced hepatotoxicity (Figure S5C). Taken together, these results indicated that the hPSC-derived HBCs have the ability to differentiate into both hepatic and biliary lineages in vitro.

### In Vivo Cell Transplantation Assays of the hPSC-Derived HBCs

To examine whether the hESC-derived HBCs could be used for hepatocyte transplantation, these cells were transplanted into $CCl_4$-treated immunodeficient mice as shown in Figure 5A. The hepatocyte functionality of the hESC-derived HBC P0 or HBC P10 was assessed by measuring secreted human ALB levels in the recipient mice (Figure 5B). Although human ALB was detected in the mice that were transplanted with the hESC-derived HBC P0 or HBC P10, it was not detected in the mice that were not transplanted with these cells. The ALB-positive cells were observed in mice transplanted with the hESC-derived HBC P0 or HBC P10 (Figure 5C). Most of the ALB-positive cells in mice transplanted with the hESC-derived HBC P10 were AFP negative (Figure 5D), indicating that transplanted hESC-derived HBCs were differentiated into mature hepatocyte-like cells (some of them were binuclear [Figure 5E, white arrows]). These results demonstrated that hESC-derived HBCs have the potential to be applied for hepatocyte transplantation.

(C) The hESC-derived cells (day 9) were plated onto a human LN111, 211, 411, or 511-coated dish. The percentage of AFP-positive cells was examined by using FACS analysis on day 9 (before passage and after passage [HBC P0]) or day 16. Data represent the mean ± SD from three independent experiments.

(D) The hESC-derived cells cultured on a human LN111-coated dish for 7 days were subjected to immunostaining with anti-AFP (green) antibodies.

(E) The hESC-derived cells (day 9) were plated onto human LN111, 211, 411, or 511-coated dishes. The gene expression levels of *AFP* and pan-hepatoblast markers (*CD133*, *EpCAM*, *CK8*, and, *CK18*) were measured by real-time RT-PCR on day 16. The gene expression levels in the hESC-derived HBCs (the LN111-attached cells were collected at 15 min after plating) were taken as 1.0.

(F) The HBCs derived from hESCs (H9) or hiPSCs (Dotcom) were cultured and cell growth was analyzed by obtaining a cell count at each passage. Data represent the mean ± SD from three independent experiments.

(G) The percentage of AFP-positive cells was examined by using FACS analysis on day 9 (before passage), P1 (HBCs passaged once), P10 (HBCs passaged ten times), and P15 (HBCs passaged 15 times). Data represent the mean ± SD from seven independent experiments.

See also Tables S2 and S3.

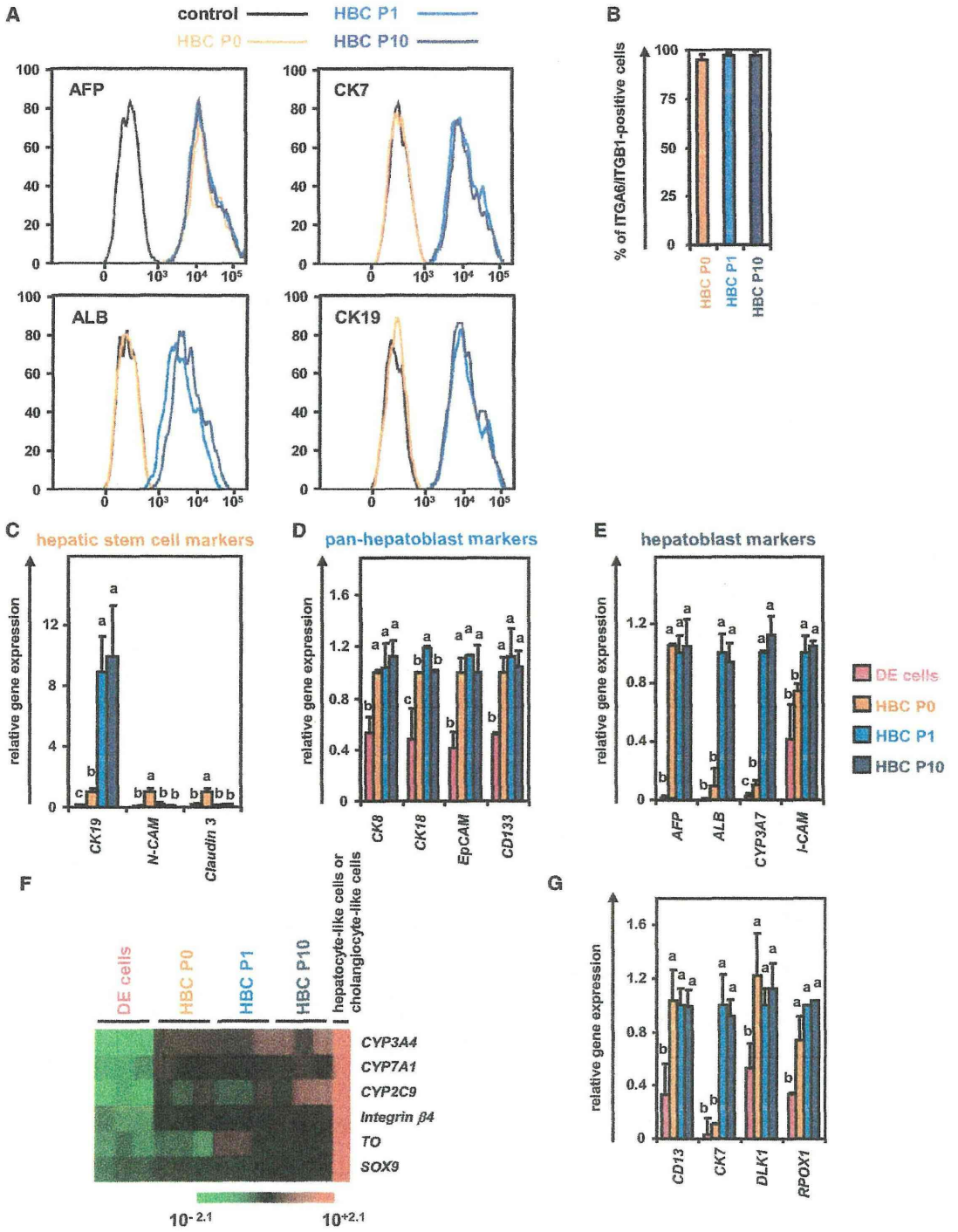


**Figure 3. The hESC-Derived HBCs Were Characterized**

(A and B) The hESCs (H9) were differentiated according to Figure 1A and then passaged onto a human LN111-coated dish. The attached cells (hESC-derived HBCs [HBC P0]) were collected at 15 min after plating. The percentage of AFP-positive, ALB-positive, CK7-positive, CK19-positive (A), and integrin α6- and integrin β1-double positive (B) cells in the hESC-derived HBC P0, HBC P1 (HBCs passaged once), and HBC P10 (HBCs passaged ten times) populations was estimated by using FACS analysis. Data represent the mean ± SD from seven independent experiments.

*(legend continued on next page)*